Neutrophil Extracellular Traps exert potential cytotoxic and proinflammatory effects in the dental pulp

Holder, Michelle; Wright, Helen; Milward, Michael; Couve, Eduardo ; Cooper, Paul

DOI:
10.1016/j.joen.2019.02.014

Document Version
Peer reviewed version

Citation for published version (Harvard):
Holder, M, Wright, H, Milward, M, Couve, E & Cooper, P 2019, 'Neutrophil Extracellular Traps exert potential cytotoxic and proinflammatory effects in the dental pulp', *Journal of Endodontics*, vol. 45, no. 5, pp. 513-520.e3. https://doi.org/10.1016/j.joen.2019.02.014

Neutrophil Extracellular Traps exert potential cytotoxic and proinflammatory effects in the dental pulp

Holder, Michelle; Wright, Helen; Milward, Michael; Cooper, Paul

Neutrophil Extracellular Traps exert potential cytotoxic and proinflammatory effects in the dental pulp

Michelle J. Holder[1], Helen J. Wright[1], Eduardo Couve[2], Michael R. Milward[1] and Paul R. Cooper[1].

[1] Oral Biology, Birmingham Dental School and Hospital, College of Medical and Dental Sciences, 5 Mill Pool Way, Edgbaston, Birmingham B5 7EG, UK

[2] Centro Interdisciplinario de Neurociencia de Valparaíso (CINV), Universidad de Valparaíso, Valparaíso, Chile Facultad de Ciencias, Universidad de Valparaíso, Valparaíso, Chile Instituto de Biología, Laboratorio de Microscopía Electrónica, Universidad de Valparaíso, Valparaíso,

The Authors deny any conflict of interest

Correspondence:
Paul R. Cooper

Oral Biology

Birmingham Dental School and Hospital

5 Mill Pool Way

Edgbaston

Birmingham, B5 7EG, UK.

Email: p.r.cooper@bham.ac.uk
Phone: +44 (01)121 466 5526

Abstract word count: 225

Total word count: 3432

Number of Figures: 4

Number of Tables: 1

Number of Supplementary Tables: 3

Number of references: 36

***Statement of Clinical Relevance (max 40 words)**

Statement of Clinical Relevance

Neutrophil extracellular traps (NETs) are present in diseased pulp. While their release is aimed at combatting bacteria the associated histones may exert cytotoxic and pro-inflammatory effects. Levels of histones may serve as prognostic and therapeutic targets in pulpal diseases.

ABSTRACT

Introduction: Neutrophil Extracellular Traps (NETs) are an important innate immune mechanism aimed at limiting the dissemination of bacteria within tissues and localize antibacterial killing mechanisms. There is significant interest in the role of NETs in a range of infectious and inflammatory disease, however, their role in diseased pulp has yet to be explored. Our aim was to determine their relevance to the infected pulp and how their components affect human dental pulp cell (HDPC) responses.

Methods: Diseased pulp tissue was stained for the presence of extracellular DNA and elastase to detect the presence of NETs. Bacteria known to infect pulp were also assayed to determine their ability to stimulate NETs. Co-culture studies and NET component challenge were used to determine the effect of extracellular NET release on HDPC viability and inflammatory response. NET-stimulated HDPC secretomes were assessed for their chemotactic activity for lymphocytes and macrophages.

Results: Data indicate that NETs are present in infected pulp tissue and whole NETs and their histone components, particularly H2A, decreased HDPC viability and stimulated chemokine release resulting in attraction of lymphocyte populations.

Conclusions: NETs likely are important in pulpal pathogenesis with injurious and chronic inflammatory effects on HDPCs, which may contribute to disease processes. Macrophages are chemo-attracted to NET-induced apoptotic HDPCs facilitating cellular debris removal. NETs and histones may provide novel prognostic markers and/or therapeutic targets for pulpal diseases.

Keywords: Pulp biology, dentine-pulp complex, inflammation, Damage-associated molecular patterns, polymorphonuclear leukocytes

INTRODUCTION

If unchecked, caries can progress to a deeper endodontic polymicrobial infection dominated by anaerobic bacteria that colonise the necrotic pulp (1,2). The pulp's innate immune responses aim to combat this infection and are orchestrated by a plethora of cytokines. Neutrophils are subsequently chemoattracted in large numbers to the diseased pulp where they provide a first line of defense (3,4,5). They can be initially primed by cytokines, complement or bacterial components in the bloodstream during infection and subsequently exhibit increased longevity at the site of infection (6). Once in the diseased pulp, neutrophils can phagocytose bacteria for intracellular killing or they can degranulate releasing reactive oxygen species (ROS) and antimicrobial proteins (AMPs), such as cathepsins, defensins, lactoferrin and lysozyme, for extracellular killing. Notably, the neutrophil trafficking process and extracellular killing mechanisms can cause significant host collateral tissue damage (7,8).

In 2004, a novel mode of neutrophil-mediated pathogen containment and killing was identified and termed neutrophil extracellular traps (NETs). NETs are extracellular web-like structures containing de-condensed nuclear chromatin adorned with antimicrobial molecules, including histones and AMPs (9). Electrostatic charge interactions between core DNA and the bacterial outer membrane are understood to enable bacterial entrapment, and killing is enabled via the co-localization of high concentrations of antimicrobial molecules (10). Induction of NETs requires complex signalling with stimuli including nitric oxide, cytokines, and Gram-positive/-negative bacterial components (11). NET release is regarded as a 'last resort' killing mechanism as it represents a form of programmed cell death, termed NETosis, resulting in the neutrophils no longer being able to undertake further killing mechanisms. Notably, NETosis is distinct from apoptosis and necrosis (10). Neutrophil ROS generation underpins the signalling for NET production and the activity of the calcium-dependent enzyme, Peptidyl Arginine Deiminase-4 (PAD4) is also essential. PAD4 citrullinates positively charged arginine residues in histones to neutrally charged citrulline enabling DNA unpackaging. Additionally, granule-derived neutrophil elastase can enter the nucleus and partially degrade histones enabling binding of MPO, which facilitates chromatin decondensation (12,13,14). The demonstration of neutrophil elastase co-localized with extracellular DNA is used to identify the presence of NETs within tissues (9). For a comprehensive review of the role of NETs in innate immunity see (11).

While NETs are aimed at protecting host tissue, they have also been associated with auto-immune and -inflammatory pathologies (15). Indeed, excessive NET release or aberrant clearance can provide a source of inflammatory and cytotoxic molecules. Recent studies have shown that NETs and their components are damaging to host cells, and in association with compromised macrophage clearance can lead to significant tissue damage. A recent review has also highlighted that histones derived from NETs act as damage-associated molecular patterns (DAMPs) and drive the pathobiology of several diseases (16).

While data derived from an animal transplant model now indicates the potential role of NETs in an infected pulpal tissue (17), there is no current information on their role in endodontic disease. This study therefore aimed to determine whether NETs are present in endodontic infections, can be induced by endodontic bacteria and their effects on human dental pulp cell (HDPC) viability and inflammatory responses.

MATERIALS & METHODS

Tissue processing and immunofluorescence of NETs in pulpitis

This study was approved by the Bioethics Committee of the Universidad de Valparaiso and complies with the recommendations of the Chilean Research Council CONICYT. Molar teeth with pulpitis were extracted with signed consentand fixed in 2% paraformaldehyde for 6h. Samples were demineralized in ethylenediaminetetraacetic acid (EDTA) (4.3%, pH 7.2) for 3 months. Following demineralization, samples were immersed in 15% followed by 30% sucrose in PBS and frozen in tissue-freezing medium (Tissue-Tek, OCT-Compound, Sakura Finetek, USA). Cryosections of 25µm were mounted on poly-L-lysine covered slides and processed for immunohistochemistry. Mounted sections were incubated for 1-hour in blocking solution and incubated overnight with 1/100 mouse anti-human neutrophil elastase monoclonal antibody (clone NP57) (Dako, Cat. Nº M0752), after PBS washes and addition of 1/500 of the secondary antibody (Alex Fluor 488 goat anti-mouse, Molecular Probes–A11029) for 1-hour. Following PBS washes sections were incubated in 1 µg/ml propidium iodide (Thermo Fisher-P1304MP) in PBS for 10 min. Tooth sections were imaged using confocal laser scanning microscope (Nikon C1 plus).

Human dental pulp cell culture

Dental pulp tissue from caries-free, intact third molar teeth, were obtained from Birmingham Dental Hospital following ethical approval (BCHC Dent334.1533.TB). Human dental pulp cells (HDPCs) were isolated via the explant procedure (18). Briefly, extracted pulpal tissue was dissected and homogenized into ~1mm^3 pieces and transferred to 25 cm^2 culture flasks containing 2 ml of α-MEM (Biosera, Worthing, UK) containing 20% fetal calf serum (FCS), 1% L-Glutamine and Amphotericin (1 µL/ml). All cultures were incubated at 37°C in a humidified atmosphere containing 5% CO_2.

HDPC cultures were exposed to a range of concentrations of histone 2A (Sigma-Aldrich, Gillingham, UK), mixed histones (H1, H2A, H2B, H3 & H4) (Roche, Burgess Hill, UK), calf thymus DNA (Sigma-Aldrich), and isolated NETs (see below) for up to 24hrs.

Quantification of NET release

Neutrophils were isolated from medically healthy volunteers (ethical approval BCHC Dent386.Tissue Bank) by discontinuous Percoll density gradient followed by ammonium chloride lysis of red blood cells (19). Neutrophils ($3x10^6$) in RPMI were incubated overnight with 1% BSA (Sigma-Aldrich) in PBS and immediately stimulated with heat-inactivated bacteria previously reported as being involved in pulpal and endodontic infections (1) at a multiplicity of infection (MOI) of 100:1; (as has previously been described (20). See ***Supplementary Table 1*** for details of the bacteria studied. A positive control of PMA (50nM) (Sigma-Aldrich) and negative control of PBS were used with a stimulation time of 4 hours. At the end of the stimulation period the media were removed and 500µl of RPMI containing 1 unit/ml MNase (Sigma-Aldrich) was added to the cells and incubated at room temperature for 10 minutes to partially digest NET-DNA. After centrifugation, the supernatant containing NETs was combined with SYTOX green nucleic acid stain (1 mM) to fluorometrically quantify the NET-DNA (Twinkle LB970; Berthold Technologies, Harpenden, UK; excitation 485 nm, emission 525 nm). Data were recorded as arbitrary fluorescent units (AFU) and converted to actual DNA amounts using a standard curve.

ATP Assay

Detection of adenosine 5´-triphosphate (ATP) was performed using the Cell Titer-Glo Luminescent Cell Viability Assay (Promega, Southampton, UK). HDPCs were trypsinised, pelleted and resuspended in culture medium prior to transfer to a white walled 96-well plate (Sarstedt, Leicester, UK). The assay was performed as per manufacturer's protocol and quantified using a luminometer (Bertholdt Technologies).

Apoptosis Assay

Detection of apoptosis was performed using the Apo-ONE Homogeneous Caspase-3/7 Assay (Promega). The assay was performed as per the manufacturer's protocol and quantified in a luminometer (Bertholdt Technologies).

Lactate Dehydrogenase Assay

Levels of Lactate Dehydrogenase (LDH) were determined using an LDH Cytotoxicity Assay Kit (Thermo Scientific, Loughborough, UK) as per the manufacturer's protocol. Absorbance was measured at 490nm and 630nm.

qPCR analysis

Total RNA was extracted from HDPC cultures using the RNeasy mini kit and reverse transcribed as per manufacturer's instructions (Qiagen, Manchester, UK). Real-time PCR was performed using the LightCycler480 (Roche) system in a final volume of 20µl containing 2µl of cDNA, 10µl SYBR green I Master PCR mix (Roche), primers at 0.5µM, and RNase/DNase free water. Primer sequences were: IL-8 (Genbank Accession No.-NM_000584.2) F-TAGCAAAAT TGAGGCCAAGG, R-GGACTTGTGGATCCTGGCTA; TNF-α (Genbank Accession No.-NM_000594.2) F-AAGAATTCAAACTGGGGCCT, R-GGCTACATGGGAACAGCCTA; Beta-2 microglobulin (NM_00048.2) F–ACCCCCACTGAAAAAGATGA, R-ATCTTCAAACCTCCATGATG. Following 5 mins denaturation at 95°C, cycling conditions were: 95°C for 20 secs, 60°C for 20 secs, and 72°C for 20 secs. All samples were amplified in duplicate and two no-template controls per primer pair were included. Expression levels were obtained from Cp values for each sample by employing the second derivative max method as computed by the LightCycler 480 software (Roche), version 1.5, with standard settings. PCR efficiency for each primer pair was determined using dilutions of sample cDNA (1:1 – 1:1000) and using the LightCycler 480 software to determine efficiency. Samples were normalised to the housekeeping gene β2-microglobulin following BestKeeper analysis (21).

qPCR array analysis

Reverse transcription of extracted RNA was performed with RT^2*Profiler* reagents (Qiagen) according to manufacturer's instructions. Eighty-four key genes mediating the human inflammatory response were simultaneously assayed with the RT^2*Profiler* PCR array (Qiagen) on a LightCycler 480 (Roche).

ELISA

Levels of Interleukin-8 (IL-8) were determined using an ELISA (Biotechne, Abingdon, UK) at 24hrs. Samples and standards were prepared following the manufacturer's instructions and analyzed on a plate reader (ELX800; Biotek, Swindon, UK).

Chemotaxis assay

Mixed lymphoctyes and monocytes were isolated from blood from medically healthy volunteers by discontinuous Percoll density gradient. Monocytes were differentiated into macrophages by cultivation with 25µg/ml granulocyte–macrophage colony-stimulating factor (GMCSF) (Generon, Slough, UK) for 7 days. Three-hundred microliters of potential chemoattractant solutions were pipetted into the wells of 96-well micro-chemotaxis plates with a 8 µm-pore size (Neuro Probe, Warwick, UK) (22). Solutions included a negative control of unsupplemented α–MEM, a positive controls of α–MEM medium containing IL-8 (Sigma, UK) or GMCSF (Generon) and test solutions of conditioned media. Primary cells were stained with 1 mg/ml calcein AM (Biotium Inc, Cambridge, UK) for 30 minutes, washed three times with PBS and resuspended in PBS. Stained cells (4×10^5) were pipetted onto the 8 µm-pore membrane in 20 µl unsupplemented medium. The chemotaxis plate was incubated at 37°C in 5% CO_2 for 3 h to allow migration. Luminescence of cells which had migrated to lower well was measured using a Twinkle LB 970 Luminometer (Berthold Technologies).

Statistical Analysis

Statistically significant differences were identified using multi-factorial analysis of variance (ANOVA) and post-hoc Tukey comparisons (95% confidence level).

RESULTS

NETs are present in infected pulp and can be stimulated by bacteria from pulpal infections

To determine whether NETs may play a role in the tooth's immune defenses, pulp tissue from teeth with pulpitis was analysed using immunofluorescence. The co-localization of elastase and DNA staining confirmed the presence of NETs. Subsequently, bacteria previously reported to infect endodontic and pulp tissues (1) (***Supplementary Table 1***) were assessed for their ability to induce NETosis. All the bacteria tested were able to stimulate significantly increased levels of NETs compared with controls (***Figure 1***).

NETs affect dental pulp cell viability

To determine whether NETs released within the pulp potentially affected viability, single and co-cultures of HDPCs (20,000 cells) and neutrophils (100,000 cells) were stimulated with PMA. Data indicated that HDPC viability was likely further reduced in the co-cultures in the presence of PMA stimulated neutrophils (***Figure 2A***). These data therefore indicated that it was appropriate to determine further whether NETs or their components decreased HDPC viability.

To determine if components of NETs may exert these effects, NETs isolated from neutrophils along with the NET components of purified DNA, histone 2A or a histone mix were used to directly stimulate HDPCs (***Figure 2B***). Data indicated that the purified NETs significantly decreased cell viability, and increased cell death and apoptosis while DNA alone exerted minimal effect. Histones, in particular 2A, were able to replicate these negative effects on HDPC viability (***Figure 2B***). Differences detected in levels of induction of cell death and apoptosis between NETs and their component histones may be a result of dosing levels and/or combined effects which occur due to histones and other NET components.

NETs modulate HDPC inflammatory response

DAMPs can stimulate an inflammatory response and hence, we assayed cytokine levels in HDPC cultures exposed to NETs and their components. Data indicated that released IL-8 levels were significantly raised in HDPC cultures following exposure to intact NETs and histones but were not raised due to DNA alone exposure. Combinations of stimuli of DNA

(calf thymus) plus histones, supported histone H2A as a key stimulus for HDPCs and indicated a dose response effect (***Figure 3A***).

To determine whether HDPCs were transcriptionally activated by NETs and their components, real-time PCR analysis was performed for IL-8 and TNF-α. Data indicated there was a temporal induction of these pro-inflammatory genes with IL-8 being induced significantly higher at the earlier 4-hour time-point while TNF-α was generally induced at higher levels by the 24-hour time-point by NETs and histones (***Figure 3B***).

To obtain more comprehensive profiling of inflammatory mediators, real-time PCR array analysis using HDPCs exposed to NETs was performed. Differential expression profiles for 12 and 16 transcripts were obtained at 4- and 24-hours post-exposure, respectively (***Table 1***), providing data which were consistent with the previous temporal differential transcript regulation identified for IL-8 and TNF-α. The importance of the role and expression level change for each individual differentially expressed gene identified would require significant undertaking therefore public database scrutiny and bioinformatics studies were undertaken (***Supplementary Tables 2 & 3***) (23). Analyses indicated that a significant proportion of the differentially expressed genes encoded for secreted chemokines/cytokines able to signal recruitment of lymphocyte populations. Subsequently, NET-activated HDPC secretomes were shown to be significantly chemotactic for whole lymphocyte and macrophages preparations compared with unstimulated controls. Notably, histone and DNA stimulation did not generate HDPC secretomes, which were chemotactically active (***Figure 4***). The HDPC stimulants when used alone were not able to recruit lymphocyte or macrophage populations (data not shown).

DISCUSSION

The identification of NETs within the infected pulp is in accord with the fact that this is clearly a conducive environment for NETosis due to the presence of bacteria and a plethora of pro-inflammatory mediators (24). In addition, AMPs such as LL-37/cathelicidin, which associate with NETs, have previously been reported in diseased pulp tissue, and can both induce and increase NET production in addition to bacterial stimulation (25). Furthermore, pulp and endodontic infections are complex and whilst the body aims to eliminate these invading bacteria, the innate immune response can also add to the tissue injury. Indeed, it is well reported that the trafficking of immune cells to sites of infection can cause break down of the tissue, while ROS and AMPs, at the levels generated during the inflammatory response, also add to the tissue insult. Similarly, whilst NETs are aimed at providing protection from infection, studies have also demonstrated that they can exert injurious tissue effects (24,26). Here, we now also demonstrate for the first time that NETs are likely to have deleterious effects in the infected pulp.

In agreement with other studies, our data supports a potential role for extracellular DAMPs in the form of histones, along with a range of other pro-inflammatory molecules, as drivers for both cell damage and local tissue induced inflammation (16]. Notably the stimulation of apoptosis in DPCs by DAMPs, as is highlighted here, would generate significant cell debris which will subsequently require removal from the tissue. Hence, it is perhaps not surprising that the dying pulp cells release chemotactic signals which concomitantly lead to the recruitment of lymphocytes, in particular macrophages, which can engulf and remove the cell debris. Notably, this efferocytotic process subsequently can shift macrophages to a M2 pro-resolving phenotype, for example by their release of lipid mediators and cytokines (27). However, in the presence of an ongoing pulpal infection, chronic inflammation would ensue and NETs would continue to further add to this milieu. In addition, the PAD4 enzyme necessary for the NETosis process, is known to be released with the nuclear NET-DNA and can citrullinate local tissue ECM components to generate autoantigens in the tissue further driving local inflammation (28).

Not surprisingly, bacteria have evolved mechanisms to avoid NET capture including DNase enzyme and polysaccharide capsule expression, as well as changes to their components, such as lipoteichoic acid modification, to decrease NET stimulation. In

agreement with this, our data demonstrate that endodontic disease-associated bacteria exhibit differential abilities to stimulate NETs. In addition, we and others have shown that many of the bacteria studied here also exhibit DNase expression and surface modifications, which enable NET avoidance (29,30,31). Combined, the expression of these virulence factors may enable endodontic-associated biofilms to evade NET capture and persist in the root canal system.

Previous studies have indicated that viral infection leads to neutrophil priming and hyper-active NET release. Indeed, recently a study using a murine lung disease model demonstrated that animals which received a dual viral and bacterial infection exhibited significantly increased mortality compared with animals which received only the viral or bacterial infection alone. Data indicated that a significant contributing factor to the tissue destruction was the exaggerated inflammatory response characterised by hyperactive neutrophilic activity in the dual infection, and in particular it was the excess NETosis, which was a key causative factor (32,33). It is conceivable that a similar process may occur in the pulp as several studies have identified evidence of viral infection in this tissue (34,35). A combined local bacterial-viral infection within the pulp would therefore likely have significant injurious effects and result in tissue, which was not salvageable or able to undertake a reparative response.

The role of DAMPs in disease due to their ability to cause tissue damage and signal inflammation is becoming increasingly evident. Histones are a form of DAMP and are highly conserved cationic proteins responsible for the packaging of nuclear DNA (15). Several cell stress-associated events have now been demonstrated to result in their extracellular discharge including apoptosis, necrosis and now more recently NETosis. When histones are released extracellularly they are detected by Toll-like receptor (TLR) family members, including TLR2, TLR4 and TLR9, present on local cell surfaces. Indeed, several TLR family members are already known to be expressed on HDPC populations (26). Receptor binding results in pro-inflammatory cytokine/chemokine release via MyD88, NFκB, NLRP3 inflammasome-dependent and Caspase-1 pathways (15). The data presented here now indicate that the histones released during NETosis exert cytotoxic and pro-inflammatory effects on HDPCs, findings which are consistent with previous studies in other cell systems. Notably, relatively high concentrations of histones have been detected in tissues from animals and patients with a range of diseases, and inadequate clearance of this form of

molecular debris by macrophages reportedly leads to their accumulation (36). It is conceivable that similar processes could also occur here, which would lead to chronic inflammation within the pulp. It is therefore important for disease resolution that macrophage chemoattraction is signalled in the pulp, as has been identified here, which will lead to the phagocytotic removal of histones and other cellular and molecular debris enabling a return to tissue homeostasis.

In conclusion, data presented here support a role for NETosis in the diseased and infected pulp. The release of the NET-DNA will also lead to the presence of DAMPs within the tissue, in the form of histones, which may also exert deleterious effect on HDPCs in the form of cytotoxicity and the stimulation of inflammatory responses. The signalling of macrophage recruitment by HDPCs may enable the removal of the cell debris, which ultimately will facilitate resolution of inflammation. Extracellular histones are now being considered as prognostic and therapeutic targets for many infectious and inflammatory disorders (15), subsequently further studies are now warranted to determine whether these molecules could be used for these purposes in the future for patients with deep caries or endodontic infections.

ACKNOWLEDGEMENTS

This study was supported by the School of Dentistry, University of Birmingham and an award to E.C. (Project number: Fondecyt 1141281/Conicyt). The authors declare no conflict of interest. We thank Professor Tony Smith (University of Birmingham) for his critical reading of the manuscript and Professor Shida Yousefi (University of Berne) for her protocols and critical advice during study development.

The authors deny any conflicts of interest related to this study.

REFERENCES

1. Narayanan LL, Vaishnavi C. Endodontic microbiology. J Conserv Dent. 2010;13:233-9.
2. Hsiao WW, Li KL, Liu Z, Jones C, Fraser-Liggett CM, Fouad AF. Microbial transformation from normal oral microbiota to acute endodontic infections. BMC Genomics. 2012;13:345-60.
3. Izumi T, Kobayashi I, Okamura K, et al. Immunohistochemical study on the immunocompetent cells of the pulp in human non-carious and carious teeth. Arch Oral Biol. 1995;40:609-14.
4. Gaudin A, Renard E, Hill M, et al. Phenotypic analysis of immunocompetent cells in healthy human dental pulp. J Endod. 2015;41:621-7.
5. Renard E, Gaudin A, Bienvenu G, et al. Immune Cells and Molecular Networks in Experimentally Induced Pulpitis. J Dent Res. 2016;95:196-205.
6. Metcalf D. Control of granulocytes and macrophages: molecular, cellular, and clinical aspects. Science. 1991;254:529-33.
7. Hager M, Cowland JB, Borregaard N. Neutrophil granules in health and disease. J Intern Med. 2010;268: 25–34.
8. Galli SJ, Borregaard N, Wynn TA. Phenotypic and functional plasticity of cells of innate immunity: macrophages, mast cells and neutrophils. Nature Immunol. 2011;12:1035–1044.
9. Brinkmann V, Reichard U, Goosmann C, et al. Neutrophil extracellular traps kill bacteria. Science. 2004;303:1532-5.
10. Brinkmann V, Zychlinsky A. Beneficial suicide: why neutrophils die to make Neutrophil extracellular traps. Nat Rev Microbiol 2007;5:577–582.
11. Cooper PR, Palmer LJ, Chapple IL. Neutrophil extracellular traps as a new paradigm in innate immunity: friend or foe? Periodontol 2000. 2013;63:165-97.
12. Li P, Li M, Lindberg MR, et al. PAD4 is essential for antibacterial innate immunity mediated by neutrophil extracellular traps. J Exp Med. 2010;207:1853–62.
13. Papayannopoulos V, Metzler KD, Hakkim A, et al. Neutrophil elastase and myeloperoxidase regulate the formation of neutrophil extracellular traps. J Cell Biol. 2010;191:677-91.

14. Palmer LJ, Chapple IL, Wright HJ, et al. Extracellular deoxyribonuclease production by periodontal bacteria. J Periodontal Res. 2012;47:439-45.

15. Hakkim A, Fürnrohr BG, Amann K, et al. Impairment of neutrophil extracellular trap degradation is associated with lupus nephritis. Proc Natl Acad Sci. 2010;107:9813-8.

16. Chen R, Kang R, Fan XG, et al. Release and activity of histone in diseases. Cell Death Dis. 2014;5:e1370.

17. Matsui A, Jin JO, Johnston CD, et al. Pathogenic bacterial species associated with endodontic infection evade innate immune control by disabling neutrophils. Infect Immun. 2014;82:4068-79.

18. Hadis MA, Cooper PR, Milward MR, et al. (2017). Development and application of LED arrays for use in phototherapy research. J Biophotonics. 2017;10:1514-25.

19. Matthews JB, Wright HJ, Roberts A, et al. Hyperactivity and reactivity of peripheral blood neutrophils in chronic periodontitis. Clin Exp Immunol. 2007;147:255–64.

20. Hirschfeld J, White PC, Milward MR, et al. Modulation of Neutrophil Extracellular Trap and Reactive Oxygen Species Release by Periodontal Bacteria. Infect Immun. 2017; 17;85-97.

21. Piehler AP, Grimholt RM, Ovstebø R, et al. Gene expression results in lipopolysaccharide-stimulated monocytes depend significantly on the choice of reference genes. BMC Immunol. 2010;11:21-34.

22. Smith JG, Smith AJ, Shelton RM, et al. Recruitment of dental pulp cells by dentine and pulp extracellular matrix components. Exp Cell Res. 2012;318:2397-2406

23. Mi H, Huang X, Muruganujan A, et al. PANTHER version 11: expanded annotation data from Gene Ontology and Reactome pathways, and data analysis tool enhancements. Nucl. Acids Res. 2016;45:D183-9.

24. Cooper PR, Chicca IJ, Holder MJ, et al. Inflammation and Regeneration in the Dentin-pulp Complex: Net Gain or Net Loss? J Endod. 2017;43:S87-S94.

25. Neumann A, Völlger L, Berends ET, et al. Novel Role of the Antimicrobial Peptide LL-37 in the Protection of Neutrophil Extracellular Traps against Degradation by Bacterial Nucleases. J Innate Immun. 2014;6:860-8.

26. Keshari RS, Jyoti A, Dubey M, et al. Cytokine induced neutrophil extracellular trap formation: implication for the inflammatory disease condition. PLoS One. 2012;7:e48111-8.

27. Korns D, Frasch SC, Fernandez-Boyanapalli R, et al. Modulation of macrophage efferocytosis in inflammation. Front Immunol. 2011;2:57-67.

28. Spengler J, Lugonja B, Ytterberg AJ, et al. Release of Active Peptidyl Arginine Deiminases by Neutrophils Can Explain Production of Extracellular Citrullinated Autoantigens in Rheumatoid Arthritis Synovial Fluid. Arthritis Rheumatol. 2015;67:3135-45.

29. LJ, Chapple IL, Wright HJ, Roberts A, et al. Extracellular deoxyribonuclease production by periodontal bacteria. J Periodontal Res. 2012;47:439-45.

30. Penas PP, Mayer MP, Gomes BP, et al. Analysis of genetic lineages and their correlation with virulence genes in Enterococcus faecalis clinical isolates from root canal and systemic infections. J Endod. 2013;39:858-64.

31. Bachtiar EW, Bachtiar BM, Dewiyani S, et al. Enterococcus faecalis with capsule polysaccharides type 2 and biofilm-forming capacity in Indonesians requiring endodontic treatment. J Investig Clin Dent. 2015;6:197-205.

32. Narasaraju T, Yang E, Samy RP, et al. Excessive neutrophils and neutrophil extracellular traps contribute to acute lung injury of influenza pneumonitis. Am J Pathol. 2011;179:199-210.

33. Narayana Moorthy A, Narasaraju T, Rai P, et al. In vivo and in vitro studies on the roles of neutrophil extracellular traps during secondary pneumococcal pneumonia after primary pulmonary influenza infection. Front Immunol. 2013;4:56-68.

34. Hernández Vigueras S, Donoso Zúñiga M, Jané-Salas E, et al. Viruses in pulp and periapical inflammation: a review. Odontology. 2016;104:184-91.

35. Zhong S, Naqvi A, Bair E, et al. Viral MicroRNAs Identified in Human Dental Pulp. J Endod. 2017;43:84-89.

36. Mena HA, Carestia A, Scotti L, et al. Extracellular histones reduce survival and angiogenic responses of late outgrowth progenitor and mature endothelial cells. J Thromb Haemost. 2016;14:397-410.

LEGENDS

Figure 1. The presence of NETs in diseased pulp tissue and stimulation by endodontic disease-associated bacteria. **A) i)** Neutrophil in a healthy molar and **ii)** NETosis in a molar with a deep caries, overlay image of **iii)** granules of elastase staining in green, and **iv)** Propidium iodide staining in red. Scale bar of 10 µm is shown. NETosis images are representative (n=3). **B)** NET production, as has previously been described (Hirschfield et al. 2017), was quantified in response to pulpal and endodontic disease-associated bacteria (1) at a multiplicity of infection (MOI) of 100:1 [see ***Supplementary Table 1*** for details of bacteria studied], PBS (negative control), and phorbol 12-myristate 13-acetate (PMA) (50 nM, positive control). NET-DNA release was quantified using Sytox Green assay and using a standard curve to obtain DNA concentrations. Data are mean ± SE (n=3). All pulpal and endodontic infection associated bacteria demonstrated statistically significant increases in NET stimulation compared with the control.

Figure 2. Potential effect of NETs and their components on HDPC viability and death. **A)** Mono- and co-cultures of HDPCs (20,000 cells) and neutrophils (100,000 cells) and in combination with the NET stimulant PMA (50 nM) showing data for viability as assessed by ATP assay. PMA induced NETosis in neutrophil mono-cultures demonstrated a decrease to 8% viability. PMA treatment in HDPC and neutrophil co-cultures resulted in an overall decrease to 15.3% viability. To achieve this decrease to 15.3% viability in these mixed cultures (containing 20,000 HDPCs and 100,000 neutrophils) then in addition to the known decrease to 8% viability of neutrophils due to PMA stimulation it can be subsequently calculated that 10,260 of the HDPC population, i.e. 51.3%, remained viable (see shaded cells in table). As PMA alone exposure of HDPCs only resulted in a decrease to 72.5% viability these data indicate that NETosis induction and the release of neutrophil components due to exposure to PMA potentially caused the additional decreased HDPC viability, i.e from 72.5% to 51.3% decreased viability in HDPC cultures. **B)** Stimulation of HDPCs with purified NETs and their components of DNA (calf thymus) and histones (H2A or mix) at the concentrations shown. Results presented are for **i)** relative viability as assessed by ATP assay, **ii)** relative cell death as determined by LDH assay, and **iii)** apoptosis induction as determined by ApoOne

assay. Data are mean ± SE (n=3). Statistical differences compared with unstimulated controls are shown: * p<0.05, **P<0.01, *** p<0.001.

Figure 3. Effect of NETs and their components on HDPC pro-inflammatory cytokine expression. **A)** IL-8 assay at 24 hours post-stimulation of culture supernatants following exposure to NETs and their components including a range of concentrations of DNA (calf thymus – 10 & 20 µg/ml) and histones (50 & 100 µg/ml), was used in combinations, to stimulate HDPC cultures. **B)** Real-time PCR analysis of **i)** IL8 and **ii)** TNF-α levels at 4 and 24 hours post-exposure to NETs (10 & 20 µg/ml), histones (2A & mix) and DNA (calf thymus). Data are mean ± SE (n=3). Statistical differences versus unstimulated controls are shown: * p < 0.05, ** P<0.01, *** p<0.001.

Figure 4. Chemotaxis assay for **A)** whole lymphocyte preparations, and **B)** macrophages, in response to HDPC stimulated secretomes. Control supernatants from HDPC cultures collected at 24 hours were unexposed while test secretomes were generated from NETs (10 µg/ml), histones [2A (100 µg/ml) & mix (100 µg/ml)] and calf thymus DNA (10 µg/ml). Positive controls for lymphocyte and macrophage chemoattraction were IL8 (25 µg/ml) and GMCSF (25 µg/ml). Results are mean ± SE (n=3). Statistical significant increases versus unstimulated HDPC control secretomes are shown: **P<0.01, *** p<0.001.

Table 1. Human Inflammatory Cytokines and Receptors RT^2 Profiler PCR Array analysis showing immune response-related transcripts with at least a 2-fold change in expression in HDPCs at **A)** 4 hours and **B)** 24 hours post-exposure to NETs. * Indicates genes present in both tables. Lighter and darker shaded background indicates genes up-regulated and down-regulated, respectively, in comparison with unstimulated HDPC control.

Supplementary Table 1. Details of the bacteria associated with endodontic and pulpal infections used for NET stimulation analysis (Narayan & Vaishnavi, 2010). A multiplicity of infection (MOI) of 100 was used for stimulation of NETs to enable comparison and for consistency with previous studies (Hirschfield et al. 2017). Bacterial strains were obtained from the American Type Culture Collection (ATCC) and the identification number is provided along with the culture conditions.

Supplementary Table 2. Analysis using the bioinformatics gene ontology tool, PANTHER (version 13.1) (Huaiyu *et al.* 2016) was used to provide molecular function, biological process, cellular compartmentalisation and protein classification data for the genes differentially expressed in HDPCs in response to NETs at 4-hours post-exposure.

Supplementary Table 3. Analysis using the bioinformatics gene ontology tool, PANTHER (version 13.1) (Huaiyu *et al.* 2016) was used to provide molecular function, biological process, cellular compartmentalisation and protein classification data for the genes differentially expressed in HDPCs in response to NETs at 24-hours post-exposure.

Figure

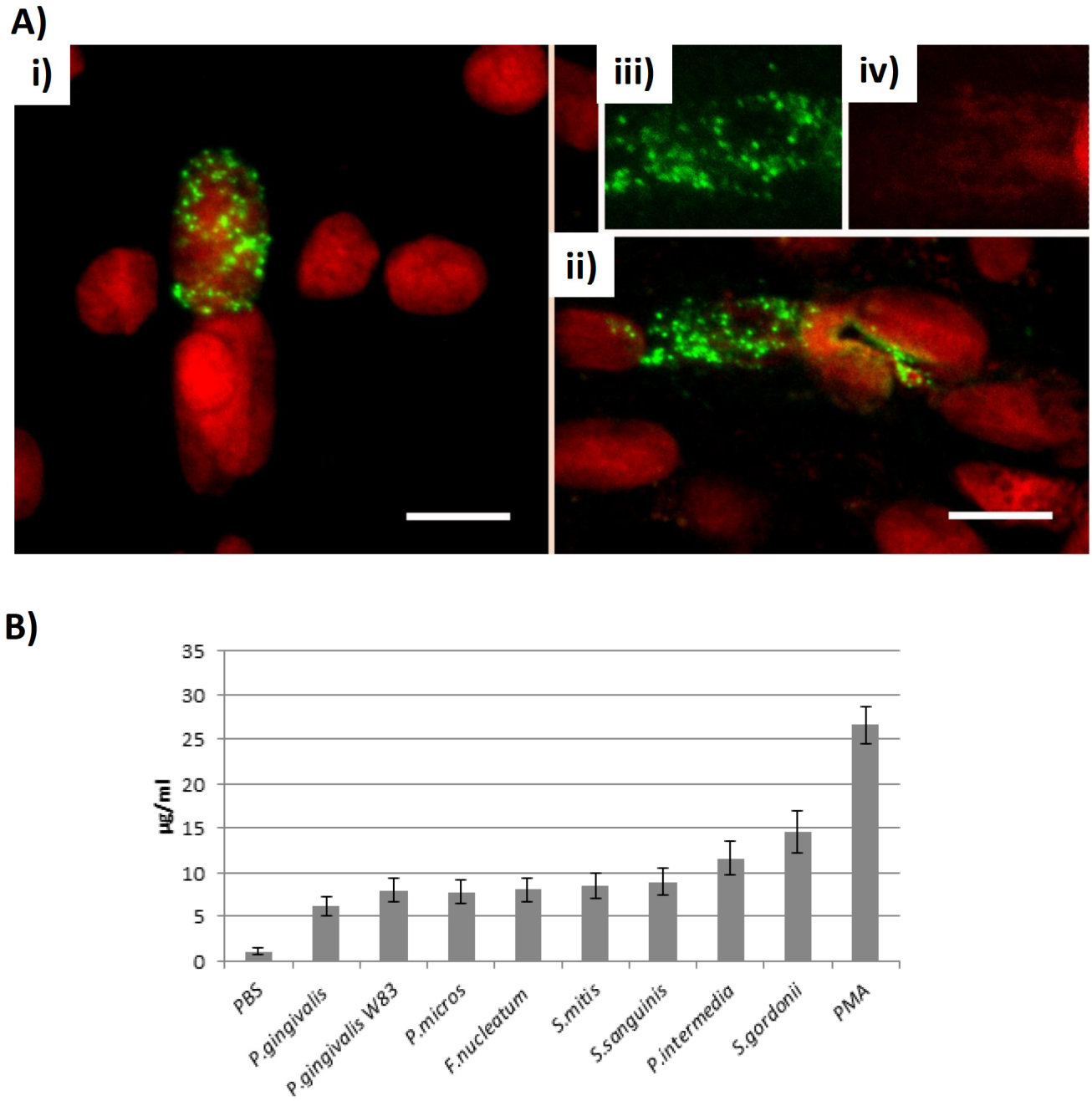
A)
i)
iii)
iv)
ii)
B)
35
30
25
20
15
10
5
0
µg/ml
PBS
P.gingivalis
P.gingivalis W83
P.micros
F.nucleatum
S.mitis
S.sanguinis
P.intermedia
S.gordonii
PMA

Fig. 1

A)

	Cellular Constituents (cell number) + PMA	% Reduction in Cell Viability	% Viable Cell Number	Number of Viable Cells	Constituent Percentages
Mono-cultures	Neutrophils (100,000)	91.9	8.1	8100	8.1
	HDPC (20,000)	27.5	72.5	14500	72.5
Co-culture	Neutrophils (100,000)	84.7	15.3	8100	8.1
	HDPC (20,000)			10260	51.3

B)

i)

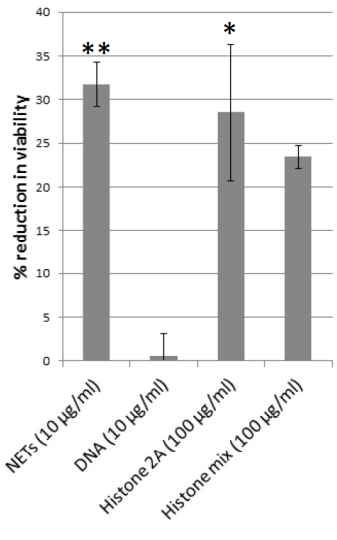

ii)

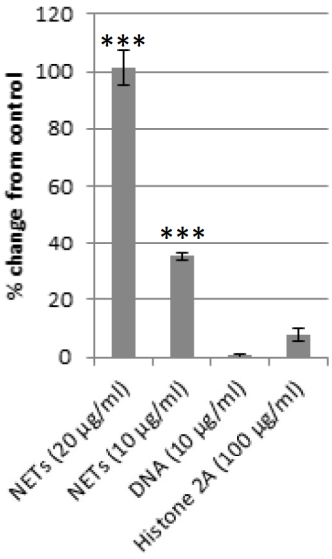

iii)

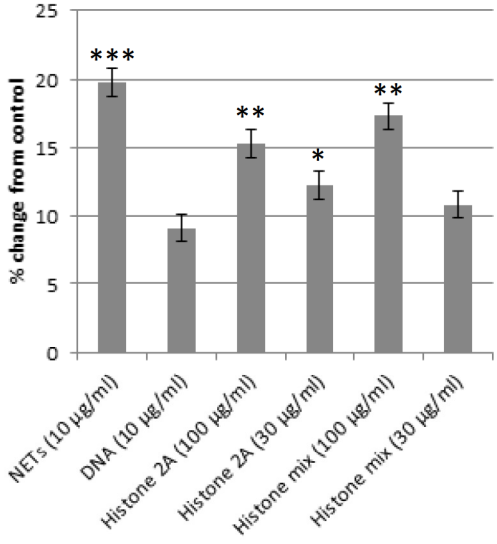

Fig. 2

A)

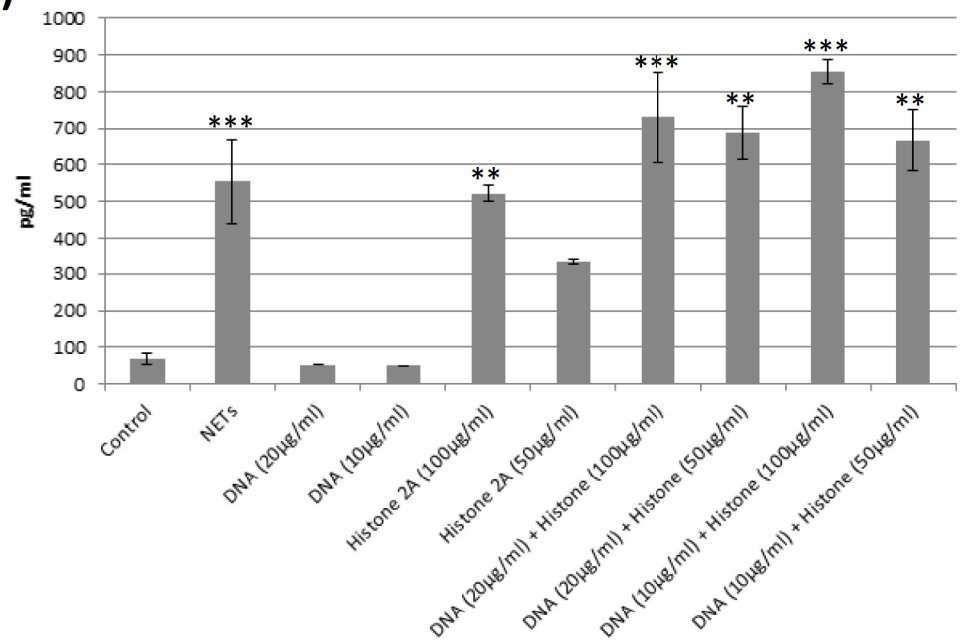
pg/ml
1000
900
800
700
600
500
400
300
200
100
0
***
***
**
***
**
**
Control
NETs
DNA (20µg/ml)
DNA (10µg/ml)
Histone 2A (100µg/ml)
Histone 2A (50µg/ml)
DNA (20µg/ml) + Histone (100µg/ml)
DNA (20µg/ml) + Histone (50µg/ml)
DNA (10µg/ml) + Histone (100µg/ml)
DNA (10µg/ml) + Histone (50µg/ml)

B)

i)

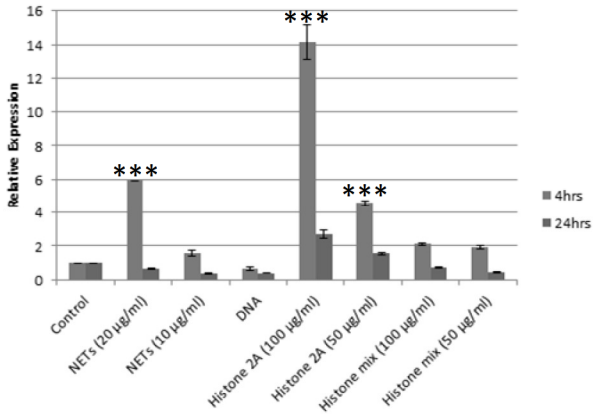
Relative Expression
16
14
12
10
8
6
4
2
0
***
***
***
4hrs
24hrs
Control
NETs (20 µg/ml)
NETs (10 µg/ml)
DNA
Histone 2A (100 µg/ml)
Histone 2A (50 µg/ml)
Histone mix (100 µg/ml)
Histone mix (50 µg/ml)

ii)

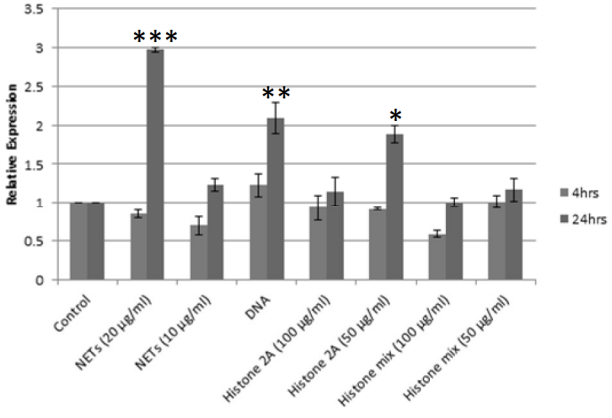
Relative Expression
3.5
3
2.5
2
1.5
1
0.5
0
***
**
*
4hrs
24hrs
Control
NETs (20 µg/ml)
NETs (10 µg/ml)
DNA
Histone 2A (100 µg/ml)
Histone 2A (50 µg/ml)
Histone mix (100 µg/ml)
Histone mix (50 µg/ml)

Fig. 3

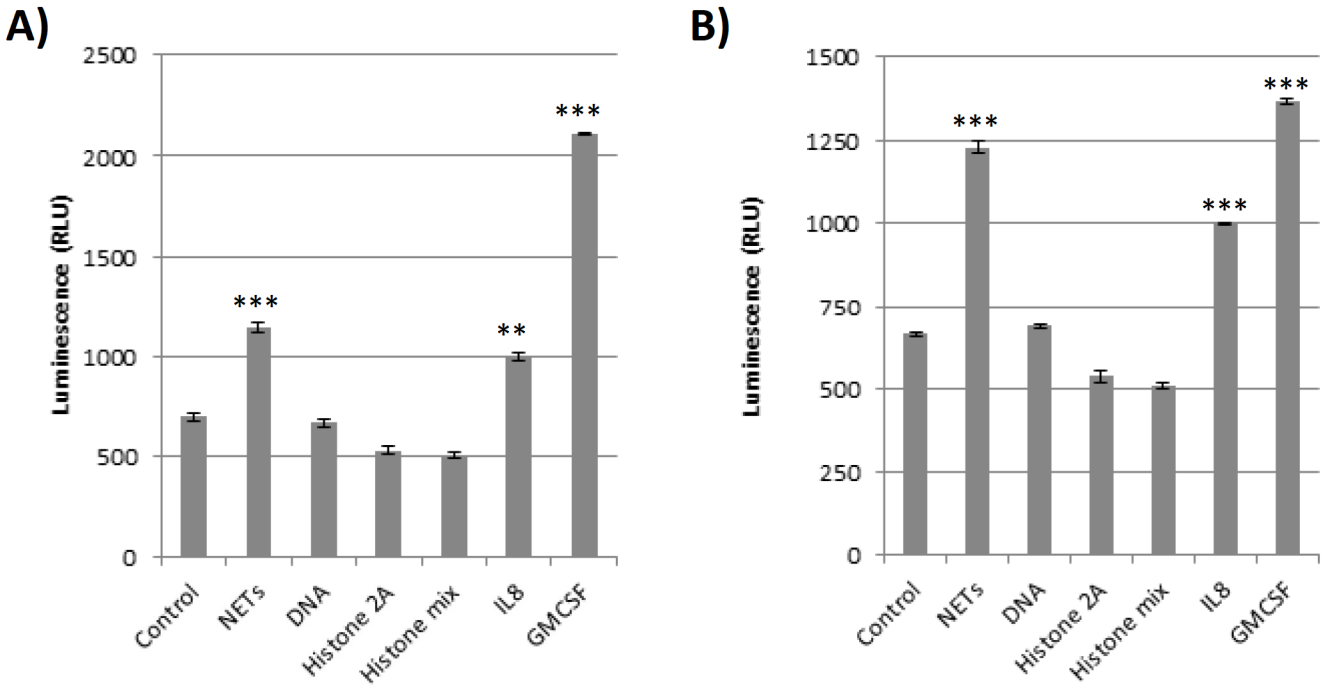
A)
Luminescence (RLU)
2500
2000
1500
1000
500
0
***
**
***
Control
NETs
DNA
Histone 2A
Histone mix
IL8
GMCSF
B)
Luminescence (RLU)
1500
1250
1000
750
500
250
0
***
***
***
Control
NETs
DNA
Histone 2A
Histone mix
IL8
GMCSF

Fig. 4

A) 4-hour post-exposure to NETs

Gene name	Gene symbol	Fold change
C-X-C motif chemokine ligand 3	CXCL3	8.75
C-X-C motif chemokine ligand 8	CXCL8	7.89
C-X-C motif chemokine ligand 2	CXCL2	6.68
Colony stimulating factor 2	CSF2	5.54
Interleukin 7	IL7	4.32
C-X-C motif chemokine ligand 1	CXCL1	4.29
Secreted phosphoprotein 1*	SPP1	2.53
Colony stimulating factor 3	CSF3	2.51
C-X-C motif chemokine ligand 9*	CXCL9	2.17
C-X3-C motif chemokine ligand 1	CX3CL1	2.10
Interleukin 9	IL9	2.00
C-C motif chemokine ligand 26	CCL26	-3.36

B) 24-hour post-exposure to NETs

Gene name	Gene symbol	Fold change
C-X-C motif chemokine receptor 2	CXCR2	10.41
Interleukin 17C	IL17C	9.06
C-X-C motif chemokine ligand 9*	CXCL9	3.66
Interleukin 27	IL27	3.51
Interleukin 13	IL13	3.14
Lymphotoxin alpha	LTA	2.71
C-X-C motif chemokine ligand 6	CXCL6	2.69
Interleukin 1A	IL1A	2.69
TNF superfamily member 10	TNFSF10	2.62
C-C motif chemokine ligand 1	CCL1	2.60
C-X3-C motif chemokine ligand 1	CX3CL1	2.48
Interleukin 17A	IL17F	2.38
TNF superfamily member 13	TNFSF13	2.10
Secreted phosphoprotein 1*	SPP1	-2.14
TNF superfamily member 4	TNFSF4	-2.27
Vascular endothelial growth factor A	VEGFA	-2.33

Table 1

Bacteria	ATCC/ID	Culture Conditions
Fusobacterium nucleatum	25586	Anaerobic
Peptostreptococcus micros	33270	Anaerobic
Porphyromonas gingivalis	33277	Anaerobic
Porphyromonas gingivalis	W83	Anaerobic
Prevotella intermedia	25611	Anaerobic
Streptococcus gordonii	10558	5% CO_2
Streptococcus mitis	49456	Anaerobic
Streptococcus sanguinis	10556	5% CO_2

Supplementary Table 1

		PANTHER GO-Slim			
	Mapped IDs	Molecular Function	Biological Process	Cellular Component	Protein Class
1	CSF3				
2	CXCL8				chemokine
3	CCL26	GTPase activity chemokine activity cytokine receptor binding pyrophosphatase activity	G-protein coupled receptor signaling pathway MAPK cascade catabolic process cellular component movement cytokine-mediated signaling pathway localization locomotion nitrogen compound metabolic process regulation of catalytic activity regulation of nucleobase-containing compound metabolic process regulation of phosphate metabolic process response to external stimulus response to interferon-gamma response to stress	extracellular space	chemokine
4	CXCL2				chemokine
5	CSF2	cytokine activity	cell differentiation	extracellular space	cytokine
6	CXCL9				chemokine
7	CXCL1				chemokine
8	IL9	interleukin-9 receptor binding	cytokine production regulation of biological process	extracellular space	
9	SPP1				
10	CXCL3				chemokine
11	CX3CL1	GTPase activity chemokine activity cytokine receptor binding pyrophosphatase activity	G-protein coupled receptor signaling pathway MAPK cascade catabolic process cellular component movement cytokine-mediated signaling pathway localization locomotion nitrogen compound metabolic process regulation of catalytic activity regulation of nucleobase-containing compound metabolic process regulation of phosphate metabolic process response to external stimulus response to interferon-gamma response to stress	extracellular space	chemokine
12	SPP1		cellular process phospholipid metabolic process		phosphatase
13	IL7				

Supplementary Table 2

		PANTHER GO-Slim			
	Mapped IDs	Molecular Function	Biological Process	Cellular Component	Protein Class
1	LTA	cytokine activity cell-cell signaling tumor necrosis factor receptor binding	cell-cell signaling cellular defense response cytokine-mediated signaling pathway immune system process induction of apoptosis		tumor necrosis factor family member
2	VEGFA	growth factor activity	anatomical structure morphogenesis angiogenesis behavior cell proliferation cellular component movement immune system process localization locomotion regulation of biological process response to abiotic stimulus response to external stimulus response to stress single-multicellular organism process transmembrane receptor protein tyrosine kinase signaling pathway	extracellular space growth factor	
3	TNFSF4	cytokine receptor binding	cell proliferation cytokine production immune system process regulation of biological process response to stress	extracellular space	tumor necrosis factor family member
4	CXCR2	G-protein coupled receptor activity apoptotic process cytokine receptor activity protein binding signal transducer activity	apoptotic process calcium-mediated signaling cellular calcium ion homeostasis cellular component movement immune response localization locomotion regulation of biological process response to external stimulus	plasma membrane	
5	IL1A				
6	CXCL6				chemokine
7	CXCL9				chemokine
8	1L13				
9	1L27	cytokine receptor binding	biosynthetic process cell differentiation cell proliferation cytokine production hemopoiesis immune response protein metabolic process regulation of biological process	extracellular space	
10	CCL1	GTPase activity chemokine activity cytokine receptor binding pyrophosphatase activity	G-protein coupled receptor signaling pathway MARK cascade catabolic process cellular component movement cytokine-mediated signaling pathway localization locomotion nitrogen compound metabolic process regulation of catalytic activity regulation of nucleobase-containing compound metabolic process regulation of phosphate metabolic process response to external stimulus response to interferon-gamma response to stress	extracellular space	chemokine
11	IL17F				
12	SPP1				
13	IL17C				
14	TNFSF13				
15	CX3CL1	GTPase activity chemokine activity cytokine receptor binding pyrophosphatase activity	G-protein coupled receptor signaling pathway MARK cascade catabolic process cellular component movement cytokine-mediated signaling pathway localization locomotion nitrogen compound metabolic process regulation of catalytic activity regulation of nucleobase-containing compound metabolic process regulation of phosphate metabolic process response to external stimulus response to interferon-gamma response to stress	extracellular space	chemokine
16	SPP1		cellular process phospholipid metabolic process		phosphatase
17	TNFSF10	cytokine activity tumor necrosis factor receptor binding	cell-cell signaling cellular defense response cytokine-mediated signaling pathway immune system process induction of apoptosis		tumor necrosis factor family member

Supplementary Table 3